

## Supplementary Information

### Engineering Semi-Permeable Giant Liposomes

Sreelakshmi Radhakrishnan<sup>a</sup>, Karthika S Nair<sup>a,b</sup>, Samir Nandi<sup>a</sup> and Harsha Bajaj<sup>\*a,b</sup>

<sup>a</sup>Microbial Processes and Technology Division, CSIR- National Institute for Interdisciplinary Science and Technology (NIIST), Trivandrum 695019, Kerala, India

<sup>b</sup>Academy of Scientific and Innovative Research (AcSIR), CSIR-Human Resource Development Centre, Ghaziabad 201002, India

\*Corresponding author E-mail: harshabajaj@niist.res.in

#### Experimental Section:

##### Materials:

1-Palmitoyl-2-oleoyl-*sn*-glycerol-3-phosphocholine powder (POPC), 1,2-diphytanyl-*sn*-glycerol-3-phosphocholine (DPhPC) and Egg PC (95%) are acquired from Avanti Polar Lipids. 1,2-dioleoyl-*sn*-glycerol-3-phosphoethanolamine labelled with ATTO 550 (ATTO 550-DOPE), 1,2-dioleoyl-*sn*-glycerol-3-phosphoethanolamine labelled with ATTO 488 (ATTO 488-DOPE), 1,2-dioleoyl-3-trimethylammonium-propane (chloride salt) (DOTAP), FITC-labelled poly-L-lysine (MW 15,000–30,000 Da), Hexokinase from *Saccharomyces cerevisiae* (EC 2.7.1.1), sucrose (≥99.5%), Mowiol 28–99% (MW 145,000 Da), magnesium chloride are from Merck. 4-(2-Hydroxyethyl)-1-piperazineethanesulfonic acid (HEPES, 99.5) is from Himedia. Alexa Fluor 350 Hydrazide (MW 350 Da), Calcein (MW 622.5 Da), Alexa Fluor 594 Hydrazide (MW 758 Da), Alexa Fluor 555 Hydrazide (MW 1150 Da), Alexa Fluor 488 Dextran (MW 3000 Da), and Alexa 488 labelling kit are procured from Thermofisher. 5-Carboxyfluorescein (FAM)-Spermine is custom synthesized by GaloreTx Pharmaceuticals Private Limited. One FAM unit is coupled to a Spermine molecule by selectively linking FAM to one of the terminal amines of Spermine. Vacuum grease from Dow Corning, Glass slides (26 mm × 76 mm, 1 mm thickness from Borosil), and coverslips (22 mm × 0.13 mm thickness) are from Blue Star.

The stock solutions of Alexa Fluor 350 (25 mM), FAM Spermine (4.3 mM), Alexa Fluor 555 (870 μM), Alexa Fluor 594 (1.3 mM), Alexa Fluor 488 Dextran (8.3 mM), Calcein (9.07mM) and FITC-PLL (10 mg/ml) are prepared in autoclaved Milli Q. Hexokinase used for labelling is prepared in phosphate-buffered saline (PBS) buffer. All the lipid stocks are prepared in chloroform.

##### Vesicle Preparation and construction of semipermeable membranes:

The vesicles are prepared using the PVA (5% w/v) gel-assisted method as described<sup>1–5</sup>. Vesicles are prepared with different lipid compositions including DPhPC, POPC, DOTAP, Egg PC, and labelled with ATTO 550-DOPE or ATTO 488. The thin lipid film is coated on a dried PVA layer and is hydrated using a buffer consisting of 100 mM HEPES, 300 mM Sucrose, and 5 mM MgCl<sub>2</sub>, pH 7. The permeability in the DPhPC + POPC vesicles is induced by incorporating DOTAP and fine-tuning the lipid compositions according to the mol% of DOTAP used. The lipid compositions used are as follows:

Sl. No	DOTAP	DPhPC	POPC	ATTO 550-DOPE/ ATTO 488-DOPE
1.	0 mol%	50 mol%	50 mol%	0.05/0.1 mol%
2.	2 mol%	49 mol%	49 mol%	0.05/0.1 mol%
3.	5 mol%	47.5 mol%	47.5 mol%	0.05/0.1 mol%
4.	10 mol%	45 mol%	45 mol%	0.05/0.1 mol%

Similarly, semipermeable vesicles are constructed using individual lipids as well:

Sl. No	DOTAP	DPhPC/POPC/Egg PC (individual lipid system)	ATTO 550-DOPE/ ATTO 488-DOPE
1.	0 mol%	100 mol%	0.05/0.1 mol%
2.	2 mol%	98 mol%	0.05/0.1 mol%
3.	5 mol%	95 mol%	0.05/0.1 mol%
4.	10 mol%	90 mol%	0.05/0.1 mol%

Altogether four different lipid systems have been tested for semi-permeable nature in presence of DOTAP including, POPC, DPhPC, Egg PC and DPhPC + POPC.

For preparing PLL encapsulated vesicles, PLL (0.45 mg/ml unlabelled and FITC-labelled PLL at 0.05 mg/mL) is added to the PVA film, followed by drying of the PVA film. The lipid mixture is then coated on top of the PVA film containing PLL. In case of Hexokinase encapsulated vesicles, the Alexa Fluor 488 labelled Hexokinase is added into the buffer that is used for lipid hydration during GUV formation.

### Imaging:

For real-time monitoring of the vesicle formation on PVA film, an EVOS epifluorescence microscope equipped with a 40× phase contrast objective with a numerical aperture of 0.65, achieving a pixel resolution of 1328 × 1048 with a 1.3 MP CMOS monochrome camera, is used. All fluorescence-based images are acquired using a Carl Zeiss Axio imager2 upright microscope with an apotome equipped with an Axiocam 503 monochrome camera with 2.83 megapixels: 1936 (H) × 1460 (V) sensor pixel count and an Olympus IX73SC inverted microscope equipped with an optiMOS camera using an objective of 20× (NA 0.8). A DAPI filter cube ( $E_x$ : 357/44;  $E_m$ : 447/60), a GFP filter cube ( $E_x$ : 470/40;  $E_m$ : 525/50), and an RFP filter cube ( $E_x$ : 550/40;  $E_m$ : 570/50) are used to capture the epifluorescence image.

### Statistical analysis:

The semi-permeable nature of the vesicle systems is investigated by understanding the permeation of 6 hydrophilic molecules namely Alexa Fluor 350 hydrazide, Calcein, FAM Spermine, Alexa Fluor 594 hydrazide, Alexa Fluor 555 hydrazide and Alexa Fluor 488 Dextran across the membranes. The vesicles that are able to transport small molecules like Alexa Fluor 350 (MW 350 Da) and do not allow the transport of large molecule like Alexa Fluor 488 Dextran (MW 3000 Da) are called as semi-permeable vesicles. Further the exact size selective nature of vesicles is determined by testing molecules of varied

sizes and charge as well. In all the vesicle systems, to quantify the transport, the concentrations of the molecules used are 500  $\mu\text{M}$  of Alexa Fluor 350, 100  $\mu\text{M}$  of Calcein, 5'FAM Spermine (17.2 $\mu\text{M}$ ), Alexa Fluor 594 (65 $\mu\text{M}$ ), Alexa Fluor 555 (8.6 $\mu\text{M}$ ) and Alexa Fluor 488 Dextran (83 $\mu\text{M}$ ).

The statistical analysis of diffusion of these molecules is obtained by quantifying the permeability in the vesicle population. The GUVs sample is mixed with the fluorescent hydrophilic molecule of interest and transferred to a BSA passivated chamber. The vesicles are incubated for 10 minutes and the images are acquired for 10-30 minutes. The images thus obtained are analyzed using Fiji software in

order to obtain the  $I_{in}/I_{out}$  as stated<sup>2</sup> where  $I_{in}$  is the fluorescence intensity inside the vesicle lumen and  $I_{out}$  is the intensity outside the lumen. In the case of GUVs containing DOTAP, the vesicles are

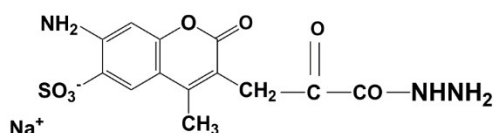
considered to be permeable if  $I_{in}/I_{out} > 0.98$  signifying the uptake of molecules in the lumen of vesicles. In the case of control GUVs (0% DOTAP), the vesicles are considered to be permeable if  $I_{in}/I_{out} > 0.95$ . The percentage of permeabilized vesicles is then analyzed and plotted using Origin.

#### **Fluorescence labelling of Hexokinase:**

The enzyme is prepared at 2 mg/mL concentration using PBS Buffer. To the enzyme, 1 M  $\text{NaHCO}_3$  is added and is transferred to a vial containing the reactive dye of choice (Alexa Fluor 488) as mentioned<sup>4</sup>. The protein-dye combination is kept at room temperature in a shaker incubator, facilitating the binding of the dye molecules to the primary amines of the enzyme. The sample is then run through a spin column at 1000g for 2 mins, and the flow through is collected in a collection tube. This step ensures that the unbound dye remains in the resin while the protein-dye combination passes through the column. The degree of labelling and the protein concentration is then determined by measuring the absorbance at 280nm and the absorbance maximum ( $\lambda_{max}$ ) of Alexa Fluor 488.

## Supporting Figures:

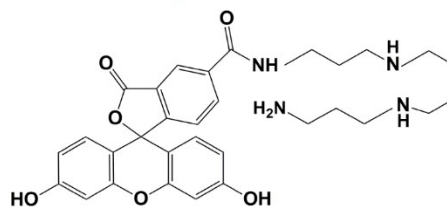
### A. Alexa Fluor 350 hydrazide



M.W: 349.29

Charge : -ve

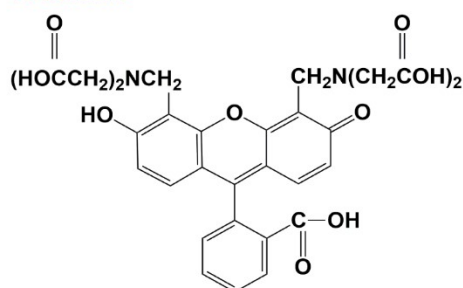
### D. 5' FAM-Spermine



M.W: 578.6

Charge : +ve

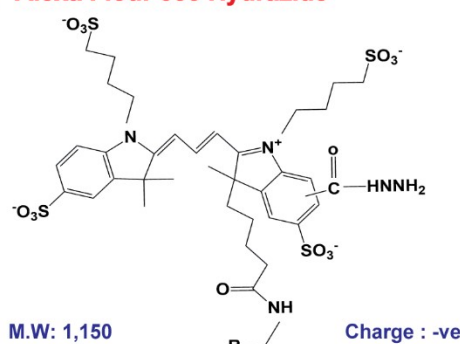
### B. Calcein



M.W: 622.5

Charge : -ve

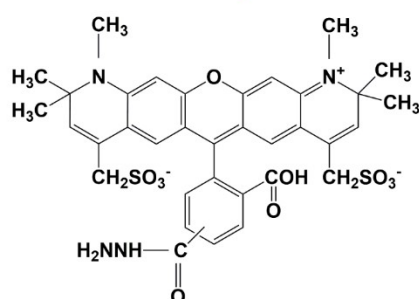
### E. Alexa Fluor 555 Hydrazide



M.W: 1,150

Charge : -ve

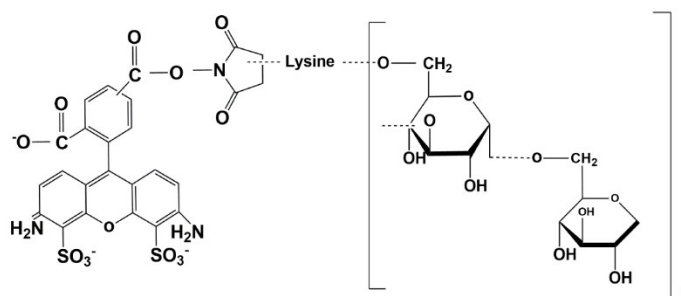
### C. Alexa Fluor 594 hydrazide



M.W: 758.79

Charge : -ve

### F. Alexa Fluor 488 Dextran



M.W: 3000

Charge : -ve

Fig. S1 Chemical structures of different fluorescent molecules used for permeability assays. Chemical structures of A) Alexa Fluor 350 Hydrazide, B) Calcein, C) Alexa Fluor 594 Hydrazide, D) 5' FAM Spermine, E) Alexa Fluor 555 Hydrazide, and F) Alexa Fluor 488 Dextran are given along with the respective Charges and molecular weight (Da).

All chemical structures are drawn using ChemDraw software. The structure references and molecular weight for Alexa Fluor 350 Hydrazide, Calcein, and Alexa Fluor 594 Hydrazide are taken directly from ThermoFisher. The reference structure for Alexa Fluor 555 Hydrazide is taken from previous studies<sup>6,7</sup>. The chemical structure of 5' FAM Spermine is drawn based on the information provided by the manufacturer. Reference for Alexa Fluor 488 Dextran chemical structure is taken from the labelling information provided at ThermoFisher.

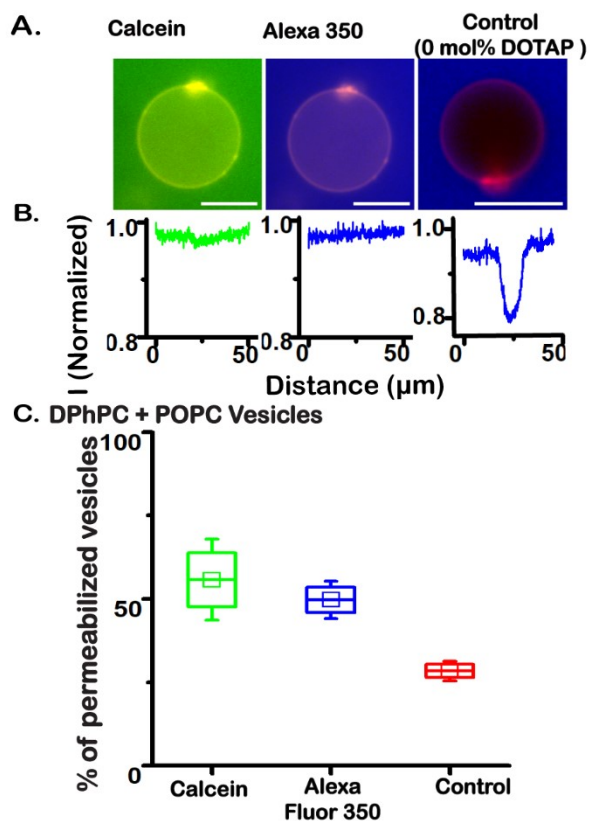


Fig. S2 (A) Single vesicle fluorescence images and (B) corresponding normalized intensities with Calcein (green) and Alexa Fluor 350 (blue) with 2 % DOTAP and without DOTAP control vesicles. (C) Statistics representing the % of Calcein ( $n= 30$  from  $N=2$  batches) and Alexa Fluor 350 permeabilization in 49 mol% DPhPC+ 49 mol% POPC+ 2% DOTAP vesicles, and in control ( $n= 80$  from  $N=2$  batches for each) vesicles. Control batches represent the transport of Alexa Fluor 350 across DPhPC + POPC vesicles that do not have DOTAP incorporated in them. The scale bar is 10  $\mu\text{m}$ . Buffer conditions: 300 mM sucrose, 5 mM  $\text{MgCl}_2$ , 100 mM HEPES at pH 7.4.

The permeabilization percentage of Calcein ( $55.8 \pm 5.8 \%$ ) and Alexa Fluor 350 ( $49.7 \pm 2.66\%$ ) in DPhPC + POPC vesicles incorporated with 2% DOTAP, exhibit a consistent trend, indicating the selective permeability of the vesicles to small molecules with molecular weights falling in the same range. In contrast, the absence of DOTAP in the vesicle system results in significantly lower permeability to Alexa Fluor 350 ( $28.4 \pm 1.6 \%$ ).

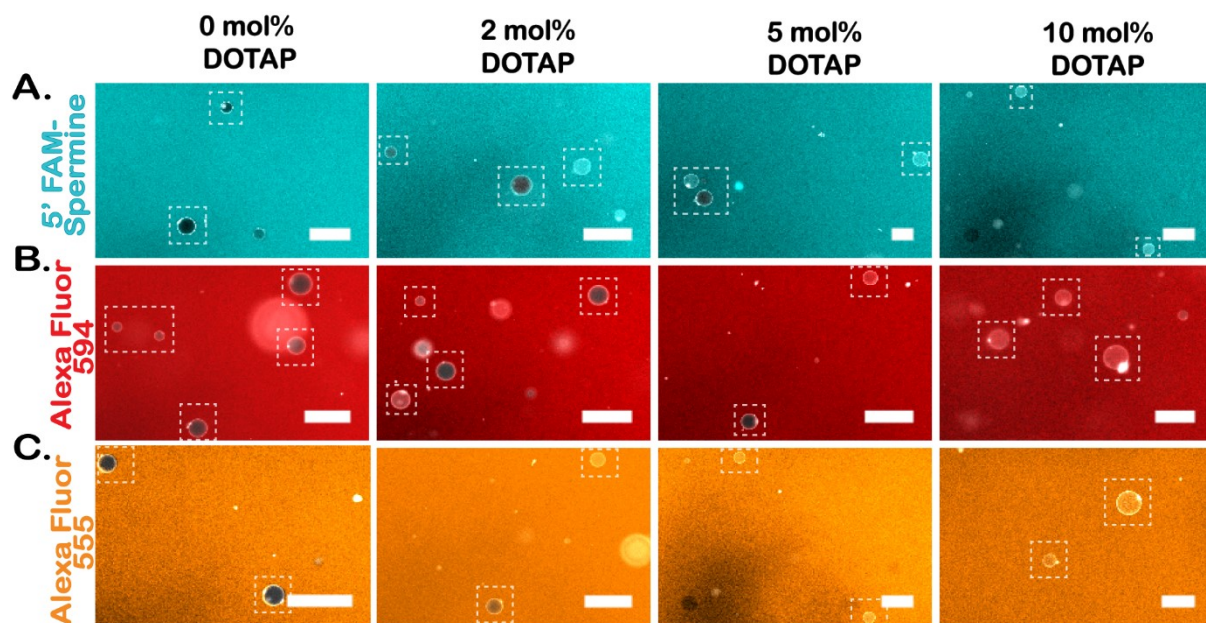
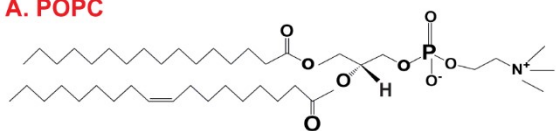


Fig. S3 Diffusion of molecules across single vesicles (DPhPC + POPC) with increasing concentration of DOTAP from 0 to 10 mol % (A) 5' FAM-Spermine (cyan) (B) Alexa Fluor 594 Hydrazide (red) and (C) Alexa 555 Hydrazide (yellow). The vesicles are highlighted by dotted boxes. The lipid membrane is represented using gray colour. The scale bar is 50  $\mu\text{m}$ . Buffer conditions: 300 mM sucrose, 5 mM  $\text{MgCl}_2$ , 100 mM HEPES at pH 7.4.

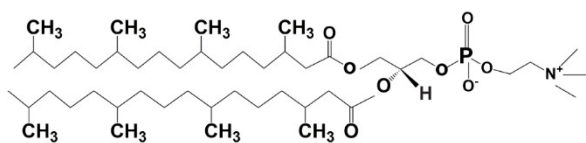
### A. POPC



Transition Temperature :  $-2^{\circ}\text{C}$

M.W: 760.12

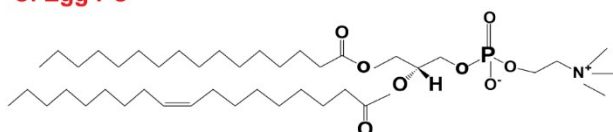
### B. DPhPC



Transition Temperature :  $-120^{\circ}\text{C} - +120^{\circ}\text{C}$

M.W: 846.25

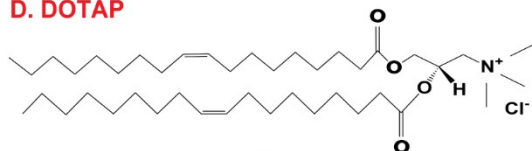
### C. Egg PC



Transition Temperature :  $-2^{\circ}\text{C}$

M.W: 770.12

### D. DOTAP



Transition Temperature :  $< 5^{\circ}\text{C}$

M.W: 698.54

Fig. S4 The chemical structure of different lipid systems used for GUV preparation. Chemical structures of A) POPC, B) DPhPC, C) Egg PC, and D) DOTAP are given along with the respective transition temperature and molecular weight (Da).

All chemical structures are drawn using ChemDraw software. The structure references, molecular weight, and transition temperatures are taken directly from Avantilipids.com.

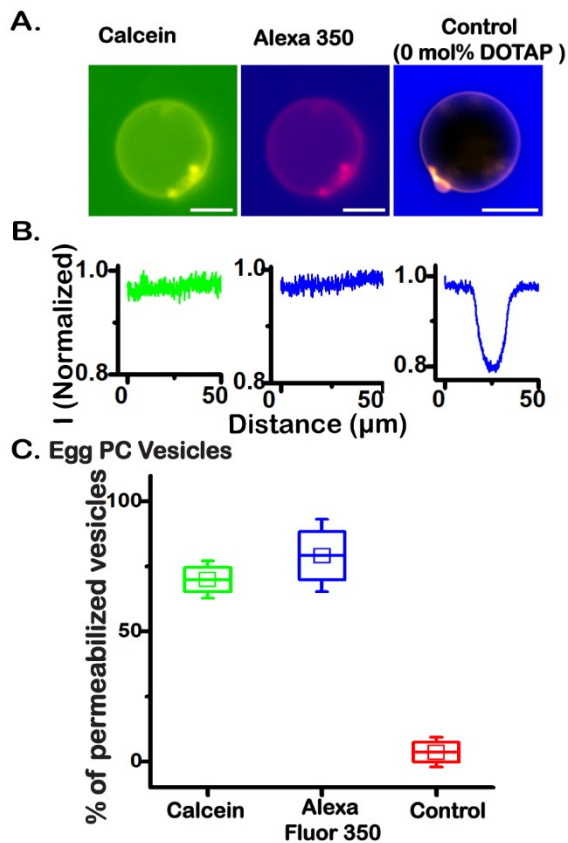


Fig. S5 (A) Single vesicle fluorescence images and (B) Normalized intensities of Calcein, Alexa Fluor 350, and Control in Egg PC + 5% DOTAP Vesicles. (C) Statistics representing the % of Calcein ( $n= 30$  from  $N=2$  batches) and Alexa Fluor 350 permeabilization in Egg PC+ 5% DOTAP vesicles, and in control ( $n= 80$  from  $N=2$  batches for each) vesicles. Control batches represent the transport of Alexa Fluor 350 across the Egg PC vesicles that do not have DOTAP incorporated in them. The scale bar is  $10 \mu\text{m}$ . Buffer conditions: 300 mM sucrose, 5 mM  $\text{MgCl}_2$ , 100 mM HEPES at pH 7.4.

The permeabilization of Calcein ( $69.9 \pm 3.4 \%$ ) and Alexa Fluor 350 ( $79.1 \pm 8.0 \%$ ) in Egg PC vesicles, incorporated with 2 mol% DOTAP demonstrates a consistent pattern indicating that the vesicle system selectively allows small molecules with molecular weights within the same range to pass through. In contrast, the absence of DOTAP in the vesicle system results in lower permeability to Alexa Fluor 350 ( $3.5 \pm 3.1\%$ ).

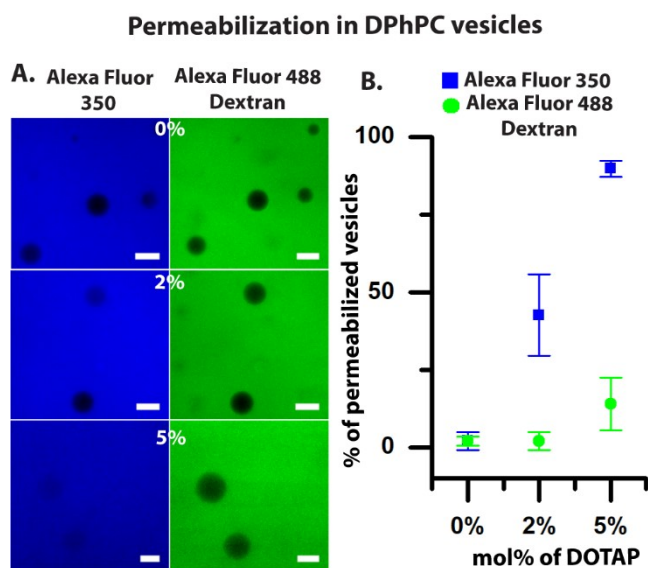


Fig. S6 Membrane permeability of DPhPC vesicles with varying membrane composition of DOTAP. (A) Fluorescence images of Alexa Fluor 350 and dextran 488 transport across vesicles with 0, 2, and 5mol% DOTAP. Scale bar: 10 $\mu$ m. (B) Statistical analysis showing the percentage of permeabilized vesicles in a population with 0% (n=50 from N=2), 2% (n=50 from N=2), and 5 mol% (n=50 from N=2) of DOTAP.

A linear and systematic increase in permeabilized vesicles against Alexa Fluor 350 with increasing DOTAP composition validates its role in creating semi-permeability in the DPhPC vesicle system. However, even with an increasing mol percentage of DOTAP, the vesicles remain impermeable to Alexa Fluor 488 Dextran, indicating the inability of large molecules to pass through the membrane.

### Permeabilization in POPC vesicles

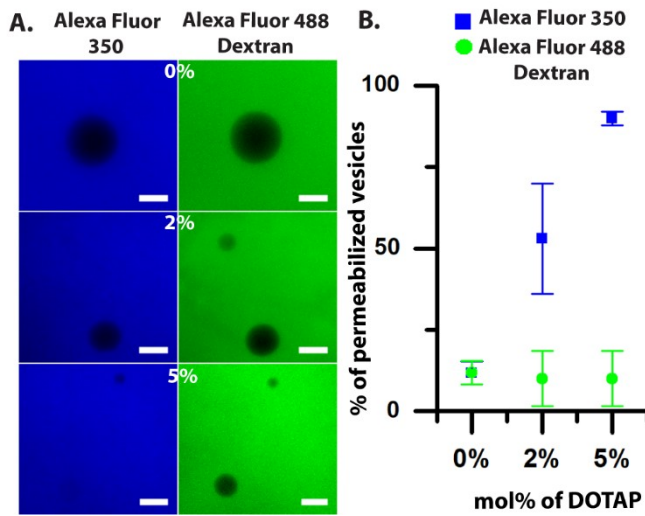


Fig. S7 Membrane permeability of POPC vesicles with varying membrane composition of DOTAP. (A) Fluorescence images of Alexa Fluor 350 and dextran 488 transport across vesicles as a function of membrane permeability in vesicles with 0, 2, and 5 mol% DOTAP. Scale bar: 10 $\mu$ m. (B) Statistical analysis showing the percentage of permeabilized vesicles in a population with 0% (n=92 from N=3), 2% (n=70 from N=3), and 5 mol% (n=50 from N=2) of DOTAP.

Similar to DPhPC vesicles, in the POPC vesicle system also the stepwise increase in DOTAP composition leads to a linear rise in the percentage of permeabilized vesicles against Alexa Fluor 350, confirming DOTAP's role in creating semi-permeability in the vesicle system. However, even with this systematic increase in DOTAP, the vesicles remain impermeable to Alexa Fluor 488 Dextran, indicating that the membrane remains impermeable to large molecules.



### Encapsulation of PLL in DOTAP vesicles

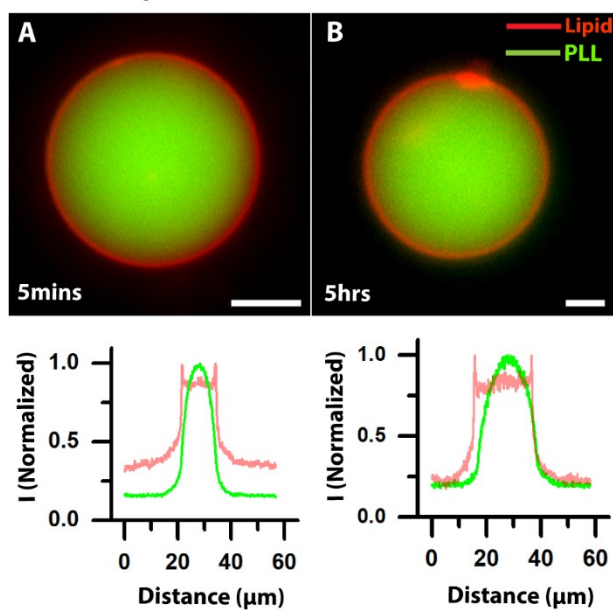


Fig. S9 Encapsulation and stability of large polymer Poly L Lysine inside DPhPC + POPC vesicles with 10mol% DOTAP over time. Vesicle with encapsulated PLL at (A) 5 mins and (B) 5 hours. The red channel represents the lipid (0.05 mol% ATTO 550 DOPE) and the green channel represents PLL (FITC-PLL). scale bar: 5 $\mu$ m. Corresponding graphs show normalized intensity profiles of PLL (Green) and lipid channel (Red).

**Supporting Table:**

Supporting Table. S1 Percentage of Alexa Fluor 350 permeabilized vesicle population with the increase in mol% of DOTAP incorporated in giant vesicles composed of different lipid systems. The values are represented as Mean  $\pm$  SD calculated from "n" number of individual vesicles and "N" the number of batches.

Lipid system	0 mol% DOTAP	2 mol% DOTAP	5 mol% DOTAP	10 mol% DOTAP
<b>DPhPC+POPC</b>	28.4 $\pm$ 1.6 n=80 N=3	51.6 $\pm$ 3.5 n=109 N=3	73 $\pm$ 5.2 n=51 N=2	92 $\pm$ 8 n=60 N=2
<b>DPhPC</b>	2 $\pm$ 2.8 n=50 N=2	42.6 $\pm$ 13.2 n=50 N=2	89.8 $\pm$ 1.9 n=50 N=2	-
<b>POPC</b>	11.6 $\pm$ 2.8 n=92 N=3	53 $\pm$ 16.9 n=70 N=3	89.9 $\pm$ 1.5 n=50 N=2	-
<b>Egg PC</b>	3.5 $\pm$ 3.12 n=70 N=3	44.5 $\pm$ 3.5 n=106 N=4	76 $\pm$ 8.2 n=83 N=4	-

Supporting Table. S2 Percentage of vesicles permeabilised by 5' FAM- Spermine, Alexa Fluor 555, and Alexa Fluor 594 with the increase in mol% of DOTAP incorporated in DPhPC+ POPC vesicle system. The number of individual vesicles investigated in the system, denoted as "n," is obtained from N= 2 batches.

Molecule	0 mol% DOTAP	2 mol% DOTAP	5 mol% DOTAP	10 mol% DOTAP
5' FAM- Spermine	13.3 $\pm$ 5.3 n=68	22.5 $\pm$ 4.0 n=69	48.4 $\pm$ 4.9 n=91	73.7 $\pm$ 0.4 n=96
Alexa Fluor 555	8.35 $\pm$ 2.4 n=50	19.2 $\pm$ 2.2 n=81	27.1 $\pm$ 6.2 n=80	60.7 $\pm$ 5.9 n=77
Alexa Fluor 594	14.3 $\pm$ 0.7 n=99	27.3 $\pm$ 1.3 n=71	58.7 $\pm$ 0.6 n=57	66.3 $\pm$ 1.04 n=98

Supporting Table. S3 Percentage of Alexa Fluor 488 Dextran permeabilized vesicle population with the increase in mol% of DOTAP incorporated in them. The values are represented as Mean  $\pm$  SD. “N” denotes the number of batches and “n” denotes the total number of vesicles .

Lipid system	0 mol% DOTAP	2 mol% DOTAP	5 mol% DOTAP	10 mol% DOTAP
<b>DPhPC+POPC</b>	9 $\pm$ 2.8 n=80 N=3	9.2 $\pm$ 0.34 n=109 N=3	15.6 $\pm$ 1.4 n=51 N=2	14.5 $\pm$ 4.5 n=60 N=2
<b>DPhPC</b>	2 $\pm$ 1.4 n=50 N=2	2 $\pm$ 2.8 n=50 N=2	14 $\pm$ 6 n=50 N=2	-
<b>POPC</b>	11.8 $\pm$ 2.9 n=92 N=3	10 $\pm$ 8.4 n=70 N=3	10 $\pm$ 6 n=50 N=2	5.8 $\pm$ 0.8 n=50 N=2
<b>Egg PC</b>	2.3 $\pm$ 3.3 n=70 N=3	10.5 $\pm$ 6.3 n=106 N=4	12.3 $\pm$ 9.2 n=83 N=4	-

## References

- 1 A. Weinberger, F. C. Tsai, G. H. Koenderink, T. F. Schmidt, R. Itri, W. Meier, T. Schmatko, A. Schröder and C. Marques, *Biophys. J.*, 2013, **105**, 154.
- 2 S. Nandi, K. S. Nair and H. Bajaj, *Langmuir*, 2023, **39**, 5891–5900.
- 3 K. S. Nair, N. B. Raj, K. M. Nampoothiri, G. Mohanan, S. Acosta-Gutiérrez and H. Bajaj, *J. Colloid Interface Sci.*, 2022, **611**, 397–407.
- 4 K. S. Nair, S. Radhakrishnan and H. Bajaj, *ACS Synth. Biol.*, 2023, **12**, 2168–2177.
- 5 G. Mohanan, K. S. Nair, K. M. Nampoothiri and H. Bajaj, *Chem. Sci.*, 2020, **11**, 4669–4679.
- 6 C. Gebhardt, M. Lehmann, M. M. Reif, M. Zacharias, G. Gemmecker and T. Cordes, *ChemPhysChem*, 2021, **22**, 1566–1583.
- 7 F. Rashid, V. S. Raducanu, M. S. Zaher, M. Tehseen, S. Habuchi and S. M. Hamdan, *Nat. Commun.*, 2019, **10**, 1–14.